Analysis of membrane pore-blocking models applied to the MF of real oily wastewaters treatment using mullite and mullite–alumina ceramic membranes

M. Abbasi[a], D. Mowla[b,c,]*

[a]*Department of Chemical Engineering, Islamic Azad University, Lamerd, Iran*
[b]*School of Petroleum and Chemical Engineering, Department of Chemical Engineering, Shiraz University, Shiraz, Iran*
[c]*Environmental Research Center in Petroleum and Petrochemical Industries, Shiraz University, Shiraz, Iran*
Tel. +98 711 2303071; Fax: +98 711 6474619; email: dmowla@shirazu.ac.ir

ABSTRACT

In microfiltration (MF) membrane processes the typical variation of the flux with time is that of initial rapid decrease followed by a long and gradual decline. The results of an experimental study regarding analysis of membrane pore-blocking models in separation of oil from oily wastewaters outlet of desalting unit of Seraje, Ghom, Iran gas wells are presented. Mullite and Mullite–Alumina (25, 50 and 75% alumina content) membranes were synthesized from kaolin clay and α-alumina powder as MF ceramic membranes. Hermia's model was used to investigate the fouling mechanisms of membranes at different time intervals (0–2.5, 0–5, 5–20, 20–120 min), and (0–120 min). It can be found that Hermia's model cannot be applied for prediction of permeation flux in any limited intervals of time since by increasing of time the filtration pore-blocking behavior changes and one model cannot predict pore-blocking behavior in all filtration time. In addition for (0–5 min) interval, maximum error of predicted permeation flux of cake filtration model is 2.96% but for (0–120 min) interval, minimum error of predicted permeation flux is 11.41%.

Keywords: Membrane fouling; Microfiltration; Ceramic membranes; Hermia's model

1. Introduction

Oily wastewaters are one of the major pollutants of the aquatic environment. This is due to the emission of a variety of industrial oily wastewaters from sources such as refineries, petrochemical plants, and transportation [1–3]. Discharge of crude oily wastewater into the sea or rivers has been under increasingly careful scrutiny in recent years. A production separator that separates most of oil from water is usually used to initially separate oil and water. The small quantity of remaining oil in water must be reduced to an acceptable limit before the water can be discharged into the sea or rivers or reinjected for water flooding [4,5]. Major pollutant in wastewater (also known as produced water) generated from oil field is oil which may range between 100 and 1,000 mg/L or more depending on demulsification efficiency and crude oil nature [6–9]. Removing oil from oil-in-water (oily water) is an important aspect of pollution control. Ceramic membranes have been known for years and

*Corresponding author.

used in many different applications depending on their numerous advantages: stability at high temperatures and pressure resistance, good chemical stability, high mechanical resistance, long life and good anti-fouling properties [10–15]. In these membranes, mullite ceramic membranes have very high chemical and thermal stability, and are very cheap because they can be prepared by extruding and calcining kaolin clay.

During membrane filtration, some constituents of feed deposit on the membrane surface and/or in the membrane matrix. There are two strategies that are usually employed to minimize the effect of fouling. The first group includes minimizing of fouling by using adequate feed pretreatment, membrane treatment, and membrane modification. The second group involves membrane remediation by chemical cleaning which is carried out to restore membrane fluxes.

Chemical agent such as NaOH, ethylene diamine tetra acetic acid disodium salt-2-hydrate, sodium dodecyl sulfate, etc have been employed. Also chemical cleaning mainly involves the dissolution of the material from the membrane surface and several factors could affect chemical cleaning process. These are: temperature, pH, cleaning time and operation conditions such as cross-flow velocity (CFV) [8].

In the last two decades, there have been a large number of studies focused on effects of operating parameters on flux decline and membrane fouling mechanisms. In these studies, membrane filtration tests under different experimental conditions were preformed to obtain data on permeates flux variation with time. Although some advances in fundamental microfiltration (MF) membrane fouling mechanisms have been achieved, further researches are needed to better understand the fouling mechanisms.

In order to enhance economy and efficiency of MF membranes, understanding the membrane fouling mechanisms is necessary for the further development. When particle size of droplets are smaller than or comparable to the membrane pores, the membrane blocking model is commonly a useful tool to explain how and when the particles to penetrate into or block the pores.

Hermia's model for prediction of permeation flux that declines in UF process with polymeric membranes are employed in Ref. [1]. In Ref. [13], performance (permeation flux, fouling resistance and Total organic carbon (TOC) rejection) of mullite and mullite–alumina ceramic MF membranes for oily wastewaters treatment has been investigated.

Now, in this research, Hermia's model [1] were used to investigate the fouling mechanisms involved in cross-flow MF of real oily wastewater at different

time intervals (0–2.5, 0–5, 5–20, and 20–120 min) and (0–120 min). The fitted results of the Hermia's model for cross-flow filtration were presented and compared with the experimental data. Also, more detailed study of the Hermia's model was provided for cross-flow filtration to explain the fouling mechanisms in MF of the real oily wastewater.

2. Materials and methods

2.1. Theory

Permeation flux, fouling resistance and TOC rejection are important parameters in design and construction of MF separation units. Permeation flux is measured gravimetrically with an electronic balance via weighting the permeate.

Permeation flux (J) is volume of permeate (V) collected per unit membrane area (A) per unit time (t):

$$J = (V/At) \tag{1}$$

Flux reduction (FR) is calculated as follows [13]:

$$FR(\%) = (J_{wi} - J_{ww}/J_{wi}) \times 100 \tag{2}$$

where J_{wi} is initial water flux before filtration and J_{ww} is water flux after filtration were measure in operating condition with a pressure of 1 bar, temperature of 25°C and cross flow rate of 1 (m s^{-1}).

TOC rejection (R) is calculated as follows:

$$R(\%) = (1 - C_p/C_f) \times 100 \tag{3}$$

where C_p represents concentration of a particular component (i.e. TOC) in permeate, while C_f is its feed concentration.

2.2. Membranes

In this research, mullite and mullite–alumina MF membranes were synthesized from kaolin clay and α-alumina powder. The kaolin material used was obtained from the Zenooz mine in Marand, Iran. Chemical analysis of the kaolin is listed in Table 1. Commercial grade of α-alumina with 99.6% purity was used to prepare the mullite–alumina membranes. The powder has an average particle size of 75 μm. Cylindrical shaped (tubular) mullite membranes (inner diameter: 9 mm, outer diameter: 14 mm and L: 30 cm) were conveniently made by extruding a mixture of about 62–69% kaolin clay and 38–31% distilled water using an extruder. The cylindrical-shaped mem-

Table 1
Chemical analysis of the kaolin clay

Component	Percent	Phases	Percent
SiO_2	61–62	Kaolinite	64
TiO_2	0.4		
Al_2O_3	24–25	Illite	2.4
Fe_2O_3	0.45–0.65		
K_2O	0.4	Quartz	27
Na_2O	0.5		
L.O.I	9.5–10	Feldspar	6.6
Total	100		100

branes were then dried at room temperature within 48 h and calcination was performed at 1,250℃ for 3 h. Free silica was removed from the calcined membranes by leaching with strong alkali solutions. Removal of this free silica increases porosity of the microporous tubular ceramic membranes. Free silica removal was carried out with aqueous solutions containing 20% by weight NaOH at a temperature of 80℃ for 5 h. Symmetric membranes were washed with distilled water for 12 h at a temperature of 80℃ in order to remove NaOH. For measurement of mullite membrane properties, three very similar membranes were selected. Properties of these membranes (water permeability, porosity, and average pore radios) had difference lower than 1%.

Porosity of the membranes measured by water absorption method before leaching was 32%, while after treatment was 41%. This test was done according to water saturation route based on the weight of absorbed water by the membrane. Porosity was obtained using the volume difference caused by floating of the membrane saturated with water in water.

Characterization of mullite membranes with mercury porosimetry method shows that average pore radius of these membranes is 0.476 µm.

Permeation flux of the mullite membranes before and after free silica removal for distillated water were 18 and 35 (L m^{-2} h^{-1}), respectively. Fig. 1 shows surface and cross-section of a synthetic mullite ceramic membrane.

Mullite–alumina membranes with 25, 50, and 75% alumina content were similarly prepared, but for improving their mechanical resistance, calcinations were carried out at 1,350℃ for 3 h.

Similar to mullite membranes, for each mullite–alumina membranes (25, 50, and 75%), three very similar membranes with difference lower than 1% in properties were selected.

Porosities of these 25, 50, and 75% alumina content membranes were 44, 49, and 56%, respectively. Permeation flux of these membranes for distillated water were 59, 109, and 582 (L m^{-2} h^{-1}), respectively. Average pore radius of mullite–alumina membranes (25, 50, and 75% alumina content) is 0.521, 0.634, and 0.728 µm respectively. Addition of alumina increases porosity and average pore diameter of the membranes because average particle size of α-alumina powder (75 µm) was larger than that of kaolin clay (25 µm). Also, sintering temperature of α-alumina (1,450–1,550°C) is higher than that of mullite (1,150℃); therefore α-alumina particles do not sinter completely at a temperature of 1,350℃.

Fig. 2 shows surface and cross-section of a synthetic 50% mullite–alumina ceramic membrane.

2.3. Process feed

Real wastewaters were used to investigate the performance of ceramic MF membranes. Outlet of the
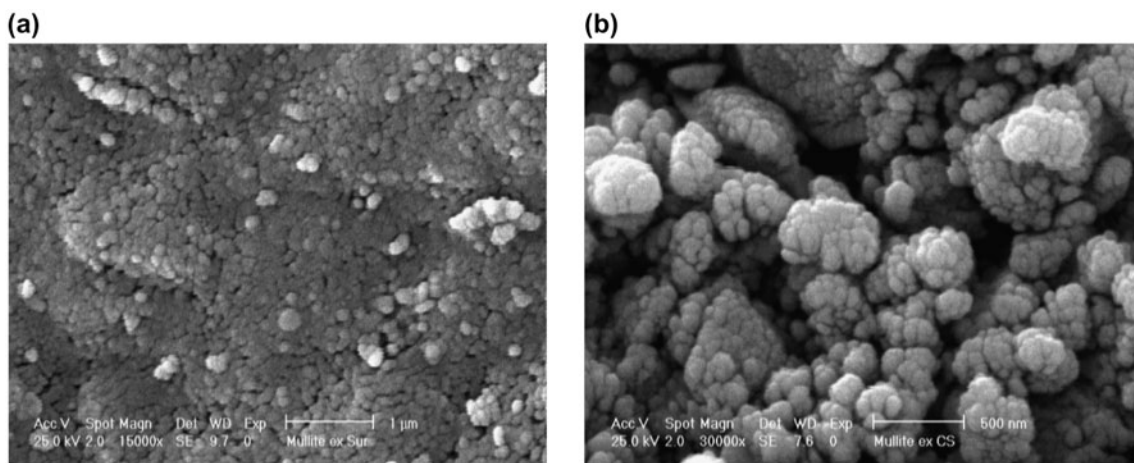
Fig. 1. SEM micrographs of the mullite membrane: (a): surface 15,000 X) and (b): cross-section 30,000 X).
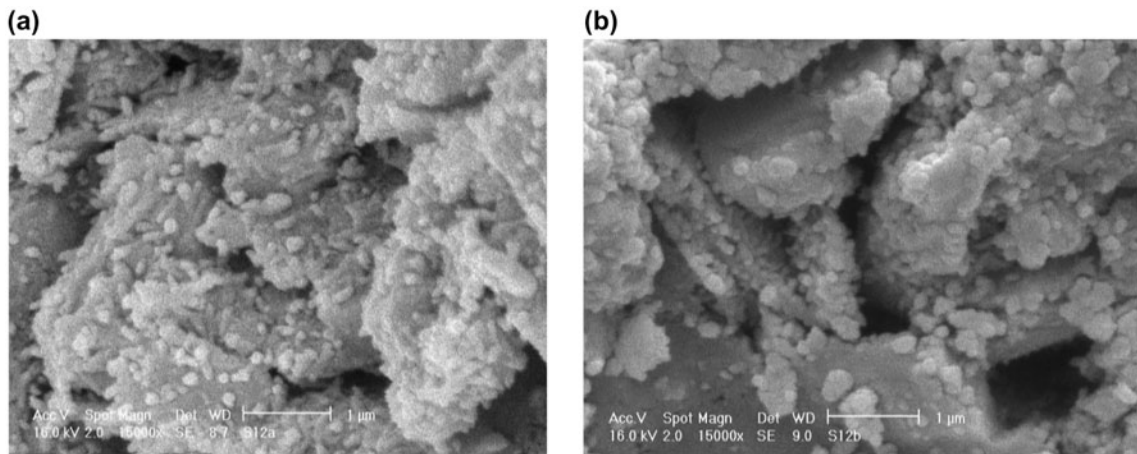
Fig. 2. SEM micrographs of the mullite–alumina (50% content) ceramic membrane: (a): surface 15,000 X and (b): cross-section 30,000 X).

desalinator unit of Seraje, Ghom gas wells was used as the real feed.

Real wastewater with high stability was taken daily and used for experiment with four membranes in three continues days, because three membrane samples of each mullite and mullite–alumina (25, 50, and 75%) membranes have been employed in experiment. In fact, in each day, four experiments carried out for treatment of daily wastewater with each mullite and mullite–alumina (25, 50, and 75%) selected membranes.

Properties of wastewater (TOC content and droplet size distribution) for all membranes were similar and also properties of real wastewater in three days did not change (difference lower than 1%).

Average TOC of this real oily wastewater was $1,060\,\mathrm{mg\,L^{-1}}$. Table 2 shows characterization of the real wastewater. Droplet size distribution of the real wastewater is shown in Fig. 3.

2.4. Setup

Fig. 4 shows the experimental setup used in all the experiments. The laboratory-scale setup was operated

Table 2
Characteristics of the real oily wastewater that has been used in experiments

Parameter	Unit
Total suspended solids	$82\,\mathrm{mg\,L^{-1}}$
Total dissolve solids	$23\,\mathrm{g\,L^{-1}}$
Chemical oxygen demand	$596\,\mathrm{mg\,L^{-1}}$
TOC	$1,060\,\mathrm{mg\,L^{-1}}$
Turbidity	$97\,\mathrm{NTU}$
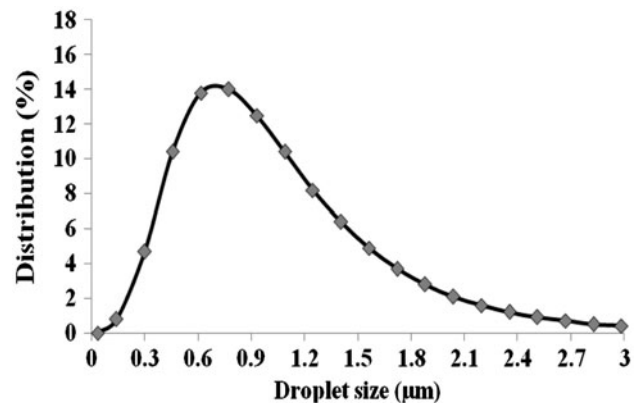
Fig. 3. Droplet size distribution of the real oily wastewaters.

in cross flow mode. The membrane surface area in contact with the feed was equal to $110\,\mathrm{cm^2}$ in the MF cell installed in the system and all the industrial reservations were considered during the experiments. The system was simple and had no complexity; however, it was designed in such a way that all important operating parameters in the MF process such as temperature, operating pressure, and volumetric flow rate could be tuned and controlled. The system mentioned above consisted of a vessel with a capacity of 10 L. This vessel had a heater to heat the feed or to keep it at a constant temperature and also a stirrer in order to keep the feed uniform. A tubular heat exchanger was used to control the feed temperature. The feed temperature was controlled with an accuracy of ±0.1°C. Temperature, pressure, and flow rate were tuned and controlled simultaneously. During the experiments, the process was carefully monitored to control CFV, pressure, and temperature. Experiments were
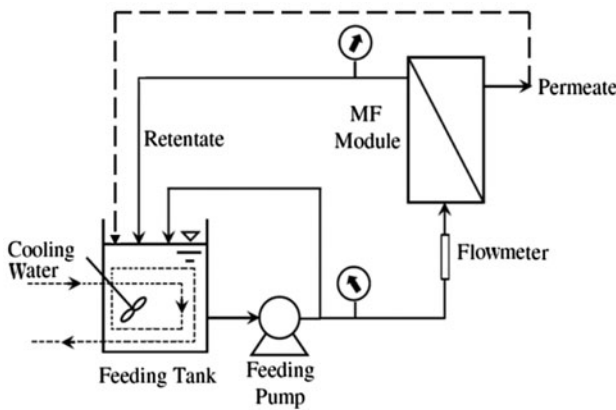
Fig. 4. Microfiltration setup.

Fig. 5. Schematic representation of blocking mechanism: (a) complete pore blocking, (b) intermediate blocking, (c) standard blocking, and (d) cake layer formation [14].

performed in total recycle mode (i.e. both permeate and retentate streams were recycled to feed tank). Permeate and retentate recycled because of oil concentration and practical size distribution of oil droplets in feed tank do nt change. Permeate after weighting are recycled to feed tank, therefore in Fig. 4, dashed line are used for stream line of recycled permeate. Process parameters during microfiltration tests are constant and do not change.

3. Modeling

In the present work, an approach followed by Hermia was used for the description of filtration phenomenon in cross-flow MF of the oily wastewater [1,9].

There are different dissolve salt such as NaCl, CaCl$_2$, and BaCl$_2$ in real wastewater that can influence fouling mechanism. Dissolve salts carry out from membranes pores and do not form cake layer on membrane surface, but can influence concentration polarization zone and decrease membrane pores diameter. This issue has been neglected because modeling of fouling becomes very difficult. Hermia's model is the most useful and applicable models for microfiltration flux decline prediction. The general equation is as follows [1,5,9,14]:

$$\frac{d^2t}{dV^2} = K\left(\frac{dt}{dV}\right)^n \tag{4}$$

where $n = 2.0$ for complete blocking; $n = 1.5$ for standard blocking; $n = 1.0$ for incomplete pore blocking (intermediate fouling) and $n = 0$ for cake filtration (see Fig. 5). The constant K has real values, but different dimensions in each case of filtration. By using Eq. (1) and derivation of permeation flux (J) with time (t), Hermia's models can be rewrite as follows:

$$\frac{dJ}{dt} = -KJ(JA)^{2-n} \tag{5}$$

After integral of this equation between times of zero and t, permeation flux change between J_0 and J and variation of J vs. t for each model can be achieved [14]. J_0 is permeation flux at beginning of filtration, so starting points of simulated and experimental data should be the same ($J = J_0$ at $t = 0$). But that the permeation flux at time equal to zero because in order to ensure precise analysis of the filtration mechanism and also to avoid unsteady state conditions, the permeate data during first 30 s of filtration process cannot be measured. If Hermia's model can predict permeation flux decline of membranes, by linearization of this models and with selection of largest (R^2), intercept and slope of line are J_0 and K respectively. Therefore, with theses fitting parameters, permeation flux at each time during filtration and fouling mechanism can be predicted.

3.1. Cake formation model

Cake/gel formation usually occurs when particles/oil droplets larger than the average pore size accumulate on the membrane surface, forming a "cake/gel." As time goes on, the cake/gel grows and provides an additional porous barrier through which the liquid must permeate. As a result, the cake/gel may increase the particles/oil droplets removal efficiency of the membrane; however, it also increases the membrane resistance and subsequently diminishes flux. For the cake filtration model, it is assumed that [1]:

(a) Shear stress is proportional to shear rate (Newtonian).
(b) All the particles/oil droplets are dimensionally similar, solute deposits on the membrane surface by superimposition forming a compressible cake/gel of uniform thickness.
(c) The resistance offered by the cake/gel is directly proportional to the volume filtered.
(d) All the particles/oil droplets are retained on the membrane surface and the flux decline phenomenon is solely dependent upon the cake/gel formation (i.e. no sealing of pores). As a result, it can be described as follows:

$$\frac{1}{J^2} = \frac{1}{J_0^2} + K_g t \tag{6}$$

where J_0 and K_g are the initial permeate flux and the constant of the cake/gel formation model, respectively [1,5,14].

3.2. Standard pore-blocking model

Standard pore block is the most dominant phenomenon when retained particles/oil droplets are dimensionally smaller than the average pore size of the membrane. It is often called adsorptive fouling or pore narrowing. In this case, particles/oil droplets in the fluid approach the membrane, enter into the pores, and adhere to the inner pore walls. Unlike the complete pore plugging model, there is no complete blocking of pores. In this case, the adhesion of particles/oil droplets to the walls decreases the available pore diameter and increases the membrane resistance. Over a period of time the pore diameter decreases and it leads to complete pore blocking. For developing the model, it is assumed that the fluid is Newtonian and only pore narrowing takes place and not complete pore blocking. Permeate flux can be obtained by the following equation:

$$\frac{1}{J^{1/2}} = \frac{1}{J_0^{1/2}} + K_s t \tag{7}$$

where K_s is the constant in standard pore blocking [1,5,14].

3.3. Complete pore-blocking model

It typically occurs when the particles/oil droplets are dimensionally similar to the mean pore size of the membrane. In this model, particles/oil droplets plug individual pores. As individual pores are plugged, the flow is diverted to other pores that plug successively. Eventually, this reduces the available membrane area and increases the membrane resistance. Due to this fact, the membrane loses its filtration performance and requires cleaning or replacement. The assumptions made for developing this model are [1]:

(a) Every particle participates in the plugging process by sealing one pore on, and once a pore is blocked, other particles/oil droplets do not enter that pore and superimpose on that particle/oil droplet (i.e. no gradual pore blocking).
(b) There is no cake formation.
(c) Feed is Newtonian.

Permeate flux can be simply represented by the following equation:

$$\text{Ln}(J) = \text{Ln}(J_0) - K_C t \tag{8}$$

where K_C is the constant in complete pore-blocking model [1,5,14].

3.4. Intermediate pore-blocking model

This model assumes each particle/oil droplet can block some membrane pores or settle on other particles/oil droplets previously blocked some other pores with superposition of particles/oil droplets. Permeate flux can be obtained by the following equation:

$$\frac{1}{J} = \frac{1}{J_0} + K_i A t \tag{9}$$

where K_i is the constant in intermediate pore-blocking model and A is membrane surface [1,5,14].

4. Results and discussion

At the best operating conditions (pressure 3 bar, CFV 1.5 (m s^{-1}) and temperature 35℃), performance of mullite and mullite–alumina membranes for treatment of real and synthetic wastewaters were compared in previous research [13].

Best operation conditions are based on largest permeation flux, because TOC rejection of homemade membranes is not very large. These membranes are suitable for pretreatment with UF membranes. Therefore, it is better to use of permeation flux for selection of best operating conditions.

Table 3 shows performance of mullite and mullite–alumina membranes for treatment of real wastewater at best operating conditions.

Table 3
Performance of the mullite–alumina ceramic membranes for treatment of the real wastewater at the best operating conditions

Membrane type	Permeation flux (Lm^{-2}h^{-1})	FR (%)	TOC rejection (%)
Mullite	41.3	46.83	84
Mullite–alumina (25% alumina)	46.8	62.31	82.2
Mullite–alumina (50% alumina)	58.1	72.63	78.7
Mullite–alumina (75% alumina)	91.5	96.27	70.8

In all experiments, fresh membranes are used and mullite and mullite–alumina membranes after experiments are not cleaned. At the end of filtration, the fouled membranes have been employed for measurement of distillated water permeation flux for calculation of FR. By addition of alumina in kaolin clay and increasing alumina content in mullite–alumina membranes, FR increased, because addition of alumina increased porosity and average pore diameter of the membranesblocking model to calculate constants. Also by increasing alumina content, adhesion energy between oil and membranes surface and pores increased. Therefore cake layer on the membrane surface becomes rigid and FR is increased. If chemical cleaning agent has been used, FR of all membranes becomes zero and there was not big difference between the flux recoveries of the various membranes. It must be noted that FR only shows fouling of membranes at the end of filtration and in fact can approximately demonstrate percent of filled membranes pores.

Because of similar properties of membrane and real wastewater properties for mullite and mullite–alumina (25, 50, and 75%) membranes, permeation flux of three membranes samples was very similar. In all figures and tables in paper, average results of three selected membranes have been presented.

For modeling, firstly, the relationship between time (*t*) and permeate flux (*J*) was drawn for all mullite and mullite–alumina membranes. In all cases, the permeate volume decreased with time. In order to ensure precise analysis of the filtration mechanism and also to avoid unsteady state conditions, the permeate data during first 30 s of filtration process was neglected. The models that were defined by Hermia for the description of various filtration laws were applied to permeate flux data that were obtained in the current studies. A linear relationship of $1/J^2$ vs. *t*, $1/J^{0.5}$ vs. *t*,

Ln (*J*) vs. *t* and $1/J$ vs. *t* was determined experimentally for cake filtration model, standard pore-blocking model, complete pore-blocking model and intermediate pore-blocking model to calculate constants (*K*) in models. To determine whether the data agree with any of the considered models, the coefficient of determination (R^2) of each plot for one model was compared with the others. Therefore, continuous lines in Figs. 6–9 show deviation of curve from linear relationship.

Variation of experimental permeation flux with time for four membranes (see Figs. 6–9) show that flux decline is very large in 5 min of filtration, in addition flux decline decrease slowly to 20 min after beginning of filtration. From 20 to 120 min of filtration, permeation flux decline of membrane decreases very slow with time. Largest permeation flux decline carry out in first 5 min of filtration. Therefore, for better prediction of permeation flux decline and better founding of fouling mechanism, this time interval divided and fouling models applied for flux decline of membrane for (0–2.5 min) interval.

In fact at beginning of filtration (0–2.5 and 0–5 min), oil droplets move to the pores of membranes and get adsorbed on pore walls and surface and fill these pores with increasing time, therefore permeation flux decreases rapidly. In future, large and medium oil droplets make a porous cake layer on the membrane surface. Therefore, fouling mechanisms has been changed during filtration and transitions of fouling mechanisms are occurred. In cake filtration mechanism, permeation flux decline is slowly because with increasing time; thickness of cake layer increase but percent of filled pores of membranes becomes approximately constant. In fact, most percent of membranes pores fill in initial times of filtration. With these physical concepts and variation of permeation flux decline with time in Figs. 6–9, for all membranes, Hermia's model was used to investigate the fouling mechanisms of membranes at different time intervals (0–2.5, 0–5, 5–20, 20–120 min) and (0–120 min).

4.1. Prediction of permeation flux by pore-blocking models for mullite membranes

As represented in Fig. 6, the Hermia's model for mullite membrane was drawn vs. time for entirely time of filtration (0–120 min). Comparing the plots for all models shows that the cake filtration model coincidence better relative to the standard pore-blocking and intermediate pore-blocking models. Results show that coefficient of determination (R^2) for cake layer formation model, intermediate pore-blocking model, standard pore-blocking model and complete
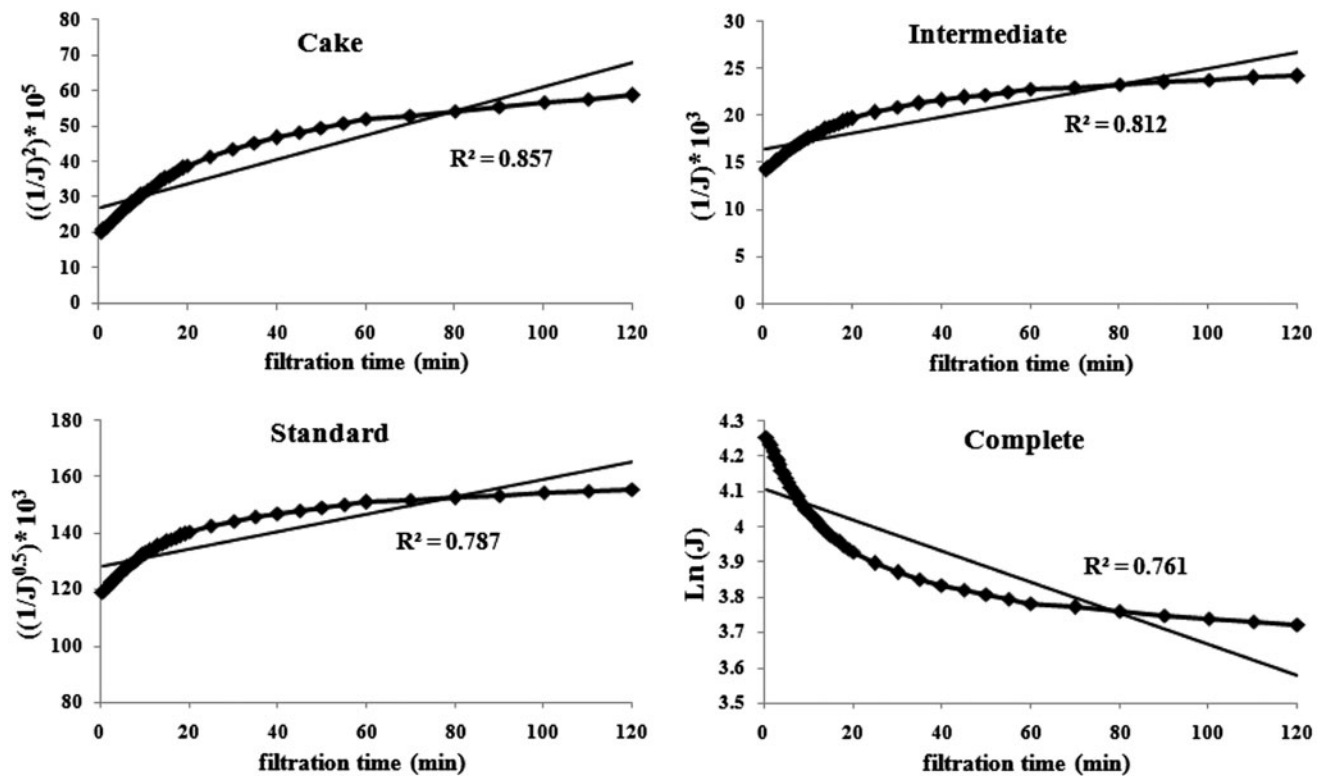
Fig. 6. R^2 value obtained by models for mullite membrane (pressure 3 bar, CFV 1.5 m/s, and temperature 35℃).

pore-blocking model are 0.857, 0.812, 0.787, and 0.761 respectively. Large deviations between experimental and predicted flux decline were observed for the complete pore-blocking model. In fact, the error of models is large, since by increasing time after beginning of filtration, pore-blocking behavior changes. Therefore, insist of entirely time (0–120 min), it is better to analysis pore-blocking behavior at short time intervals.

For modeling of FR, the Hermia's model for mullite membrane was drawn vs. time for different intervals and the coefficient of determination (R^2) of each plot for one model was calculated and listed in Table 4. Results show that standard and complete pore-blocking models can predict flux of permeate better than cake filtration model at first times of filtration (0–2.5 and 0–5 min). By increasing time to 20 min, results indicate that cake filtration model predict flux decline better than other models because the best coefficient of determination (R^2) is larger than other models. For (20–120 min) interval results is similar to (5–20 min) interval. Therefore it can be conclude that after 2.5 min of collecting of permeate, pores of mullite membranes becomes fill and cake layer formed and it become thicker by increasing time. By comparing particle size distribution of oil droplet (see Fig. 3) and mean average pore diameter of mullite membranes

(0.476 μm), it can be found that diameter of oil droplets is larger than average pore diameter of mullite membranes and a large percent of oil droplets cannot inter into mullite pores. Of course at first time interval (0–2.5 min), membrane surface is clean and pores of membrane is empty, therefore small oil droplet enter into membranes pore and complete the pores. After filling of membrane pores, large oil droplets make a cake layer on the membrane surface by increasing time.

4.2. Prediction of permeation flux by pore-blocking models for mullite–alumina membranes

Figs. 7–9 illustrate modeling of flux decline for mullite–alumina membranes for entire time of filtration (0–120 min). The results show that the fitting of models with experimental data is not as good as mullite ceramic membrane. Largest deviations between experimental and predicted flux decline of mullite–alumina membranes were observed for the complete blocking model. The cake filtration model predict flux decline of mullite–alumina membrane better than other models because the cake layer fouling mechanism occurs when particles/oil droplets are much greater than the membrane pore size. Consequently,
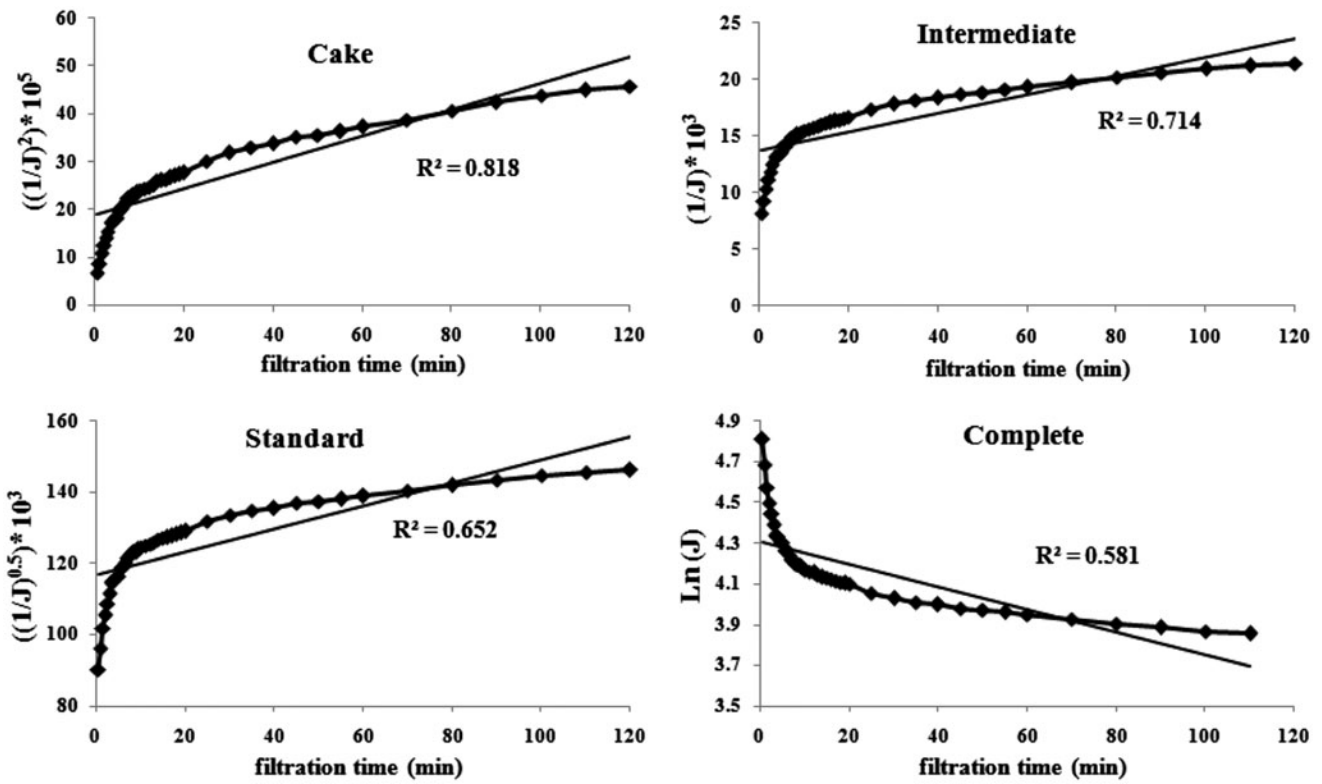
Fig. 7. R^2 value obtained by models for mullite–alumina (25% alumina content) membrane (pressure 3 bar, CFV 1.5 m/s, and temperature 35℃).
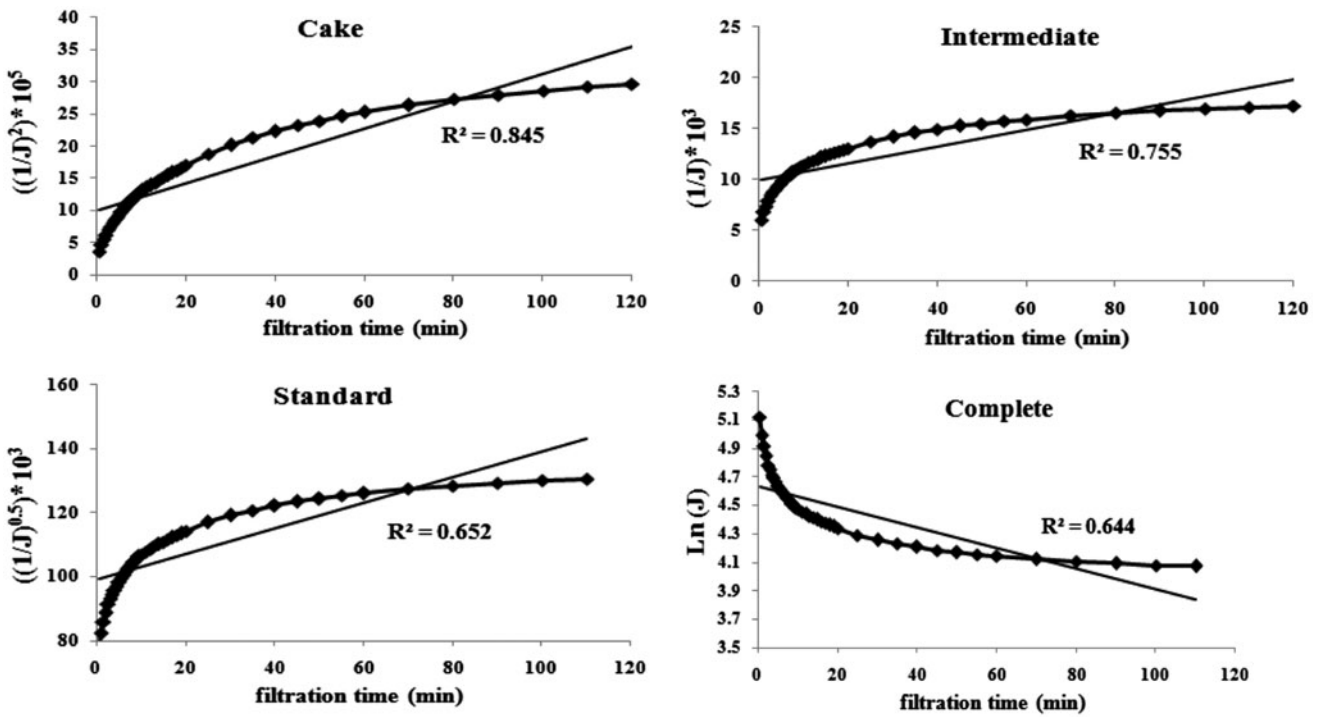
Fig. 8. R^2 value obtained by models for mullite–alumina (50% alumina content) membrane (pressure 3 bar, CFV 1.5 m/s, and temperature 35℃).
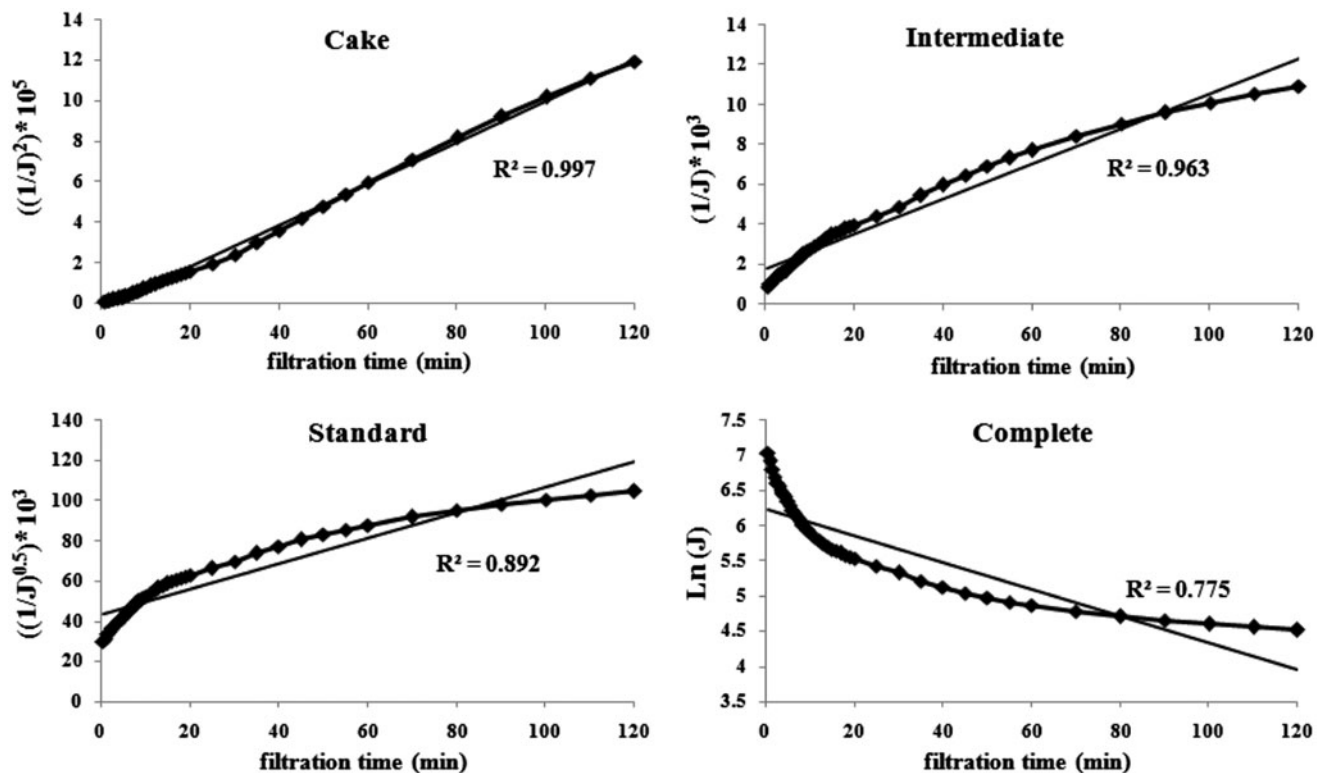
Fig. 9. R^2 value obtained by models for mullite–alumina (75% alumina content) membrane (pressure 3 bar, CFV 1.5 m/s, and temperature 35°C).

they are unable to enter the membrane pores. Some of the main factors that have an influence on the cake layer resistance are: oil droplets deformation, cake compression, and cake layer thickness [14]. Similar to mullite membranes, for decreasing error of models, different time intervals selected and summary of results for each membrane are listed in Tables 5–7.

As shown in Table 5 for mullite–alumina membrane (25% alumina), cake filtration model is best model for prediction of FR. By employing Hermia's model for different time intervals, the best coefficient of determination (R^2) of cake filtration model increases from 0.818 to at least 0.922 for (5–20 min) interval.

Results in Table 6 indicate that similar to mullite–alumina membrane (25% alumina), cake filtration model has larger the best coefficient of determination (R^2) to another models at different time intervals. By increasing the time intervals, the best coefficient of determination (R^2) of cake filtration model decreases since number of experimental data and time increase, therefore largest (R^2) is for first time interval (0–2.5 min).

For mullite–alumina membrane (75% alumina), results in Table 7 show that for first time interval (0–2.5 min), intermediate pore-blocking model have largest accuracy but for (0–5 min) interval and other

Table 4
The best coefficient of determination (R^2) of models for prediction of permeation flux with time for mullite membranes at different time intervals

Models	0–2.5 (min)	0–5 (min)	5–20 (min)	20–120 (min)	0–120 (min)
Cake filtration	0.995	0.999	0.993	0.925	0.857
Intermediate pore blocking	0.996	0.999	0.987	0.91	0.812
Standard pore blocking	0.997	0.999	0.984	0.901	0.787
Complete pore blocking	0.997	0.999	0.981	0.893	0.761

intervals cake filtration models predict flux decline better than other models. Therefore, it can be concluded that after 2.5 min of collecting of permeate, pores of mullite membranes becomes fill and the cake layer is formed. For 25 and 50% alumina content in mullite–alumina membranes, cohesive energy between oil and membrane surface causes that cake layer to be formed at first time interval (0–2.5 min), but for 75% alumina mullite–alumina membranes, the average pore diameter of membrane is increased and small oil droplets enter in to large membrane pores and cake do not form on the membrane surface at first time interval (0–2.5 min).

4.3. Comparison of predicted permeation flux by pore-blocking models for mullite and mullite–alumina membranes

Table 8 illustrates comparison of models for different membranes for entirely filtration time. The results show that for all membrane, cake filtration model has the best coefficient of determination (R^2) compared to other models but only for mullite–alumina (75% alumina content) prediction is acceptable. For better comparison of the models, average prediction errors of models are calculated. For this purpose, by using the experimental data, average value of models constant (K) are calculated and replaced in Eqs. (2–5). Therefore, average error at different times for predicted flux and actual flux are determined. Tables 9 and 10 show

average error of models for prediction of permeation flux for two intervals (0–5 and 0–120 min), respectively. By comparisons of these tables, it can be stated that model of Hermia cannot be used for prediction of the permeate flux, in the limited range of time, since during the whole process duration one model cannot predict the all of occurring filtration mechanisms. In addition for (0–5 min) interval, the maximum error of predicted permeation flux of cake filtration model is 2.96% but for (0–120 min) interval, the error of predicted permeation flux is large and the obtained results are not well acceptable because the minimum error of predicted permeation flux is 11.41%.

In final, it can be said that droplet size distribution in permeate can support (or conflict with) many of the hypotheses of fouling mechanisms regarding the time-course of pore-blocking and cake build-up. Although the analyzing of membrane pore-blocking models using particles size distribution of permeates is very difficult. Because at different times of filtration, particle size distribution are changed and also differences between they are low. In addition, comparison of membrane fouling models with droplet size distribution of oil in permeates become qualitative not quantitative because there are not a formula between oil droplet distribution of permeate and membrane fouling models. Unfortunately, authors have not particle size distribution of permeates, because of economical problems (at least 48 samples of permeate for size distribution must be analyzed using particles size analyzer).

Table 5
The best coefficient of determination (R^2) of models for prediction of permeation flux with time for mullite–alumina (25% alumina content) membranes at different time intervals

Models	0–2.5 (min)	0–5 (min)	5–20 (min)	20–120 (min)	0–120 (min)
Cake filtration	0.995	0.948	0.922	0.976	0.818
Intermediate pore blocking	0.987	0.923	0.906	0.965	0.714
Standard pore blocking	0.981	0.908	0.897	0.958	0.652
Complete pore blocking	0.974	0.89	0.888	0.95	0.581

Table 6
The best coefficient of determination (R^2) of models for prediction of permeation flux with time for mullite–alumina (50% alumina content) membranes at different time intervals

Models	0–2.5 (min)	0–5 (min)	5–20 (min)	20–120 (min)	0–120 (min)
Cake filtration	0.996	0.976	0.975	0.919	0.845
Intermediate pore blocking	0.988	0.953	0.961	0.897	0.755
Standard pore blocking	0.982	0.938	0.952	0.885	0.652
Complete pore blocking	0.975	0.921	0.944	0.873	0.644

Table 7
The best coefficient of determination (R^2) of models for prediction of permeation flux with time for mullite–alumina (75% alumina content) membranes at different time intervals

Models	0–2.5 (min)	0–5 (min)	5–20 (min)	20–120 (min)	0–120 (min)
Cake filtration	0.994	0.997	0.998	0.997	0.997
Intermediate pore blocking	0.999	0.986	0.983	0.975	0.963
Standard pore blocking	0.998	0.974	0.967	0.951	0.892
Complete pore blocking	0.996	0.958	0.945	0.918	0.775

Table 8
The best coefficient of determination (R^2) of models for prediction of permeation flux with mullite and mullite–alumina membranes

Membrane	Cake filtration model	Intermediate pore blocking model	Standard pore blocking model	Complete pore blocking model
Mullite	0.857	0.812	0.787	0.761
Mullite–alumina (25% alumina)	0.818	0.714	0.652	0.581
Mullite–alumina (50% alumina)	0.833	0.728	0.652	0.644
Mullite–alumina (75% alumina)	0.997	0.963	0.892	0.775

Table 9
Average error of models for prediction of permeation flux (0–5 min)

Membrane	Cake filtration model (%)	Intermediate pore-blocking model (%)	Standard pore-blocking model (%)	Complete pore-blocking model (%)
Mullite	1.46	1.38	1.32	1.09
Mullite–alumina (25% alumina)	2.96	4.28	5.12	6.53
Mullite–alumina (50% alumina)	1.97	2.94	3.86	5.04
Mullite–alumina (75% alumina)	2.32	3.94	3.24	3.88

Table 10
Average error of models for prediction of permeation flux (0–120 min)

Membrane	Cake filtration model (%)	Intermediate pore-blocking model (%)	Standard pore-blocking model (%)	Complete pore-blocking model (%)
Mullite	11.41	13.76	14.99	17.46
Mullite–alumina (25% alumina)	42.30	55.24	61.5	68.21
Mullite–alumina (50% alumina)	35.76	50.95	58.74	68.89
Mullite–alumina (75% alumina)	15.45	35.73	78.40	133.40

5. Conclusions

In this research, mechanisms of flux decline of synthetic mullite and mullite–alumina (25, 50, and 75% alumina content) membranes for treatment of a real wastewater were investigated. For this purpose, Hermia's model was used in different time intervals (0–2.5, 0–5, 5–20, 20–120 min) and (0–120 min).

The coefficient of determination (R^2) of each case was compared between the Hermia's model. According to the obtained results, it can be concluded that the best fit to experimental data is for the cake layer formation model for all the ceramic membrane tested for entirely filtration time (0–120 min). After cake filtration model, the best flux predicted to the experimental data was intermediate pore-blocking model and the worst predicted flux was for complete pore-blocking model. Results show that error of models is not low, because by increasing time after beginning of filtration, pore-blocking behavior is changed. Therefore, insist of entirely time analysis of pore-blocking behavior must be carried out at short time intervals. Results show that complete pore-blocking model can predict flux of permeate better than cake filtration model at first times of filtration (0–2.5 min) for mullite membrane. Also For mullite–alumina membrane (75% alumina), results show that for first time interval (0–2.5 min), intermediate pore-blocking model have largest accuracy. In final, it can be concluded that after 2.5 min of collecting of permeate, pores of mullite, and mullite alumina membranes becomes fill and cake layer is formed and becomes thicker by increasing time therefore cake filtration model can applied for prediction of flux.

Nomenclature

A	—	membrane area (m²])
C	—	concentration (mg L^{-1})
CFV	—	cross-flow velocity (m s^{-1})
d_p	—	diameter of oil droplets (m)
FR	—	flux reduction (–)
L	—	tubular membrane length (m)
J	—	filtration flux (L m^{-2} h^{-1})
J_0	—	initial filtration flux (L m^{-2} h^{-1})
K_C	—	complete pore-blocking model constant (s^{-1})
K_g	—	cake filtration model constant (s m^{-6})
K_i	—	intermediate pore-blocking model constant (m^{-3})
K_s	—	standard pore-blocking model constant (s^{-3})
n	—	blocking index and compressibility coefficient (–)
P	—	pressure (bar)
J	—	permeation flux (L m^{-2} h^{-1})
J_{wi}	—	water flux before filtration (L m^{-2} h^{-1})
J_{ww}	—	water flux after filtration (L m^{-2} h^{-1})
R	—	rejection of TOC (–)
t	—	filtration time (s)
T	—	temperature (℃)

References

[1] J. Hermia, Constant pressure blocking filtration laws application to power law: Non-Newtonian fluids, Trans. Inst. Chem. Eng. 60 (1982) 183–187.

[2] B. Chakrabarty, A.K. Ghoshal, M.K. Purkait, Ultrafiltration of stable oil-in-water emulsion by polysulfone membrane, J. Membr. Sci. 325 (2008) 427–437.

[3] A. Salahi, T. Mohammadi, A. Rahmatpour, F. Rekabdar, Oily wastewater treatment using ultrafiltration, Desalin. Water Treat. 6 (2009) 1–10.

[4] C.Y. Tang, Y. Peng, Fouling of ultrafiltration membrane during secondary effluent filtration, Desalin. Water Treat. 30 (2011) 289–294.

[5] A. Salahi, M. Abbasi, T. Mohammadi, Permeate flux decline during UF of oily wastewater: Experimental and modeling, Desalination 251 (2010) 153–160.

[6] M. Abbasi, A. Salahi, M. Mirfendereski, T. Mohammadi, A. Pak, Dimensional analysis of permeation flux for microfiltration of oily wastewaters using mullite ceramic membranes, Desalination 252 (2010) 113–119.

[7] S. Kosvintsev, R.G. Holdich, I.W. Cumming, V.M. Starov, Modeling of dead-end microfiltration with pore blocking and cake formation, J. Membr. Sci. 208 (2002) 181–192.

[8] T. Mohammadi, M. Kazemimoghadam, Chemical cleaning of ultrafiltration membrane in the milk industry, Desalination 204 (2007) 213–218.

[9] A.B. Koltuniewiz, R.W. Field, Process factors during removal of oil-in-water emulsions with cross-flow microfiltration, Desalination 105 (1996) 79–89.

[10] T. Furukawa, K. Kokubo, K. Nakamura, K. Matsumoto, Modeling of the permeate flux decline during MF and UF cross-flow filtration of soy sauce lees, J. Membr. Sci. 322 (2008) 491–502.

[11] L. Zheng, C. Huaqiang, D. Bingzhi, S. Fei, L. Hao, Pretreatment to enhance flux of ultrafiltration membrane, Desalin. Water Treat. 30 (2011) 80–88.

[12] K.G. Hwang, C.Y. Liao, K.L. Tung, Effect of membrane pore size on the particle fouling in membrane filtration, Desalination 234 (2008) 16–23.

[13] M. Abbasi, M. Mirfendereski, M. Nikbakht, M. Golshenas, T. Mohammadi, Performance study of mullite and mullite–alumina ceramic MF membranes for oily wastewaters treatment, Desalination 259 (2010) 169–178.

[14] M.C.V. Vela, S. Blanco, Analysis of membrane pore blocking models applied to the ultrafiltration of PEG, Sep. Purif. Technol. 62 (2008) 489–498.

[15] L. Zhao, W. Xia, H. Zhao, Z. Xu, X. Wu, J. Zhao, Modeling and membrane resistance analysis of stainless steel ultrafiltration membrane in alkali wastewater recovery processing, Desalin. Wat. Treat. 30 (2011) 80–88.